Chemosphere 78 (2010) 1121–1128

Contents lists available at ScienceDirect

Chemosphere

journal homepage: www.elsevier.com/locate/chemosphere

Monitoring structure and activity of nitrifying bacterial biofilm in an automatic biodetector of water toxicity

Andrzej Woznica [a,*], Agnieszka Nowak [a], Claudia Beimfohr [b], Jerzy Karczewski [c], Tytus Bernas [d,e]

[a] Department of Biochemistry, Faculty of Biology and Environmental Protection, University of Silesia, 40-032 Katowice, Poland
[b] Vermicon AG, Emmy Noether Str. 2, 80995 Münich, Germany
[c] Department of Biophysics, Faculty of Biology and Environmental Protection, University of Silesia, 40-032 Katowice, Poland
[d] Department of Plant Anatomy & Cytology, Faculty of Biology and Environmental Protection, University of Silesia, 40-032 Katowice, Poland
[e] Department of Physiology and Medical Physics, RCSI, Dublin 2, Ireland

ARTICLE INFO

Article history:
Received 17 June 2009
Received in revised form 11 December 2009
Accepted 14 December 2009
Available online 21 January 2010

Keywords:
Biofilm maturation
Nitrifying bacteria
Verhulst model
FISH
ABTOW

ABSTRACT

Automatic biodetector of water toxicity is a biosensor based on monitoring of catalytic activity of the nitrifying bacteria. To create a standardized biosensing system, development of the biofilm must be characterized to determine the prerequisites for its biological (biocatalytic) stability. In this paper, growth of biofilm comprising ammonium-oxidizing bacteria (AOB) and nitrite-oxidizing bacteria (NOB) in the open cellular polyurethane material polyurethane sponge bioreactor has been investigated.

Dynamics of the biofilm formation was estimated using AOB and NOB metabolic activity and the volume occupied by these two types of bacteria in the biofilm. Spectrophotometry liquid ion chromatography and image cytometry were used, respectively, for these measurements. A mathematical model of the dynamics of biofilm formation was established. These data indicate that open cellular polyurethane material is a good basis for the immobilization of nitrifying bacteria. Moreover, growth of the biofilm leads to its stable structural form, whose biocatalytic activity (12.29 for AOB and 6.84 μmol min^{-1} for NOB) is constant in the long term.

1. Introduction

A release of anthropogenic toxins to the environment results in a growing need for environmental monitoring. The use of biosensing for that purpose permits simultaneous detection of diverse chemical components that contribute to overall toxicity level in water. There are several commercially available biosensing systems, based on luminescent marine bacteria (Microtox), plankton organisms (Daphtoxkit F, Protoxkit F, Algaltoxkit F) (Christensen et al., 1992; Pessala et al., 2004; Kahru et al., 2008), molluscs (*Unio tumidus*, Symbio) and fishes (*Gnathonemus petersii*). Despite their obvious usefulness, these systems have certain limitations. First, their response time is usually long (from 24 h to several days), with the exception of systems using bacteria as the sensing element. Second, they may require a number of samples (with the exception of systems based on higher organisms) and therefore do not permit in situ measurements. In order to solve these problems and create system for fast, continuous estimation of water toxicity, in situ may apply nitrifying bacteria as a sensing element.

Nitrification is a multi-stage biological transformation of reduced forms of nitrogen to nitrate. The nitrification reactions are catalyzed by two groups of ubiquitous lithoautotrophic bacteria. The first group comprises ammonium-oxidizing bacteria (AOB), and the second group comprises nitrite-oxidizing bacteria (NOB) (Hovanec et al., 1998; Bothe et al., 2000; Gieseke et al., 2001; Koops and Pommerening-Röser, 2001; Kowalchuk and Stephen, 2001; Mota et al., 2005). In aquatic environments, genera of both AOB and NOB have been observed exclusively in the form of flocs or biofilms.

Use of nitrifying bacteria for biosensing is motivated by their high sensitivity (Ilzumi et al., 1998; König et al., 1998; Cui et al., 2005) to a wide range of toxins, including phenols (Ilzumi et al., 1998; König et al., 1998), cyanides (Kim et al., 2008) and heavy metals (Chandran and Love, 2008; Park and Ely, 2008). Moreover, the nitrifying bacteria have natural ability to form biofilms (Liu and Tay, 2001). Thus, unlike other bacteria used as active elements of biodetectors (Bang et al., 2001; de Ory et al., 2004) and biosensors (Blum, 1997; Bettaieb et al., 2007), they do not require artificial immobilization. Therefore, we present a biosensor based on consortia of nitrifying bacteria immobilized on a porous carrier (polyurethane) to detect the presence of toxins in flowing water. The bacteria were immobilized during growth by the formation of complexes of surface-associated cells enclosed in a matrix of extracellular polymeric substances (EPS) (Wimpenny et al., 2000). The biofilm is usually populated together by the two groups

* Corresponding author. Tel.: +48 322009576; fax: +48 322009361.
E-mail address: andrzej.woznica@us.edu.pl (A. Woznica).

0045-6535/$ - see front matter © 2009 Elsevier Ltd. All rights reserved.
doi:10.1016/j.chemosphere.2009.12.035

of bacteria (catalyzing two stages of nitrification), linked by mutualistic interactions. Composition and spatial architecture of such biofilms are, in general, non-uniform and may vary in time. Therefore, to create a standardized biosensing system, the development of the biofilm must be characterized to determine the prerequisites for its biological (biocatalytic) stability. In other words, conditions in which the biofilm stability will be maintained by its natural homeostasis have to be established. We have applied spectrophotometry, ion chromatography and image cytometry complemented by computed X-ray tomography (Al-Raoush and Willson, 2005; Xi et al., 2006). Furthermore, we described the biofilm development using a mathematical model (Diaz et al., 1999; Lokshina et al., 2001; Tsoularis and Wallace, 2002; Fujikawa et al., 2004; van Impe et al., 2005; Liu, 2006; Peleg et al., 2007).

2. Materials and methods

In our experiment, biofilm growth in the automatic biodetector of water toxicity (ABTOW) bioreactor with high ammonium level was examined. Non-buffered mineral medium was used for that purpose. Ammonium concentration and pH were corrected daily to 7.6 mM and 7.5 units, respectively. The medium was continuously aerated (4 L min^{-1}). Velocity of medium laminar flow was 0.0037 m s^{-1} in order to simulate natural slow flow of the surface water. In the OCPM, we observed process of biofilm maturation on form growing on the polyurethane arm or caught in the node of sponge.

2.1. Bacterial culture

Consortia of nitrifying bacteria were used. Bacteria were isolated from activated sludge from water treatment plant Klimzowiec, Katowice, Silesia (Woznica et al., 2006). Consortia of nitrifying bacteria had grown in 2 L laboratory scale reactor as a fed-batch culture in Braun Melsulgen Biostat in 1.5 L mineral liquid medium (MacDonald and Spokes, 1980). Reactor was aerated continuously 2 L min^{-1}, and the oxygen concentration was about 5 mg L^{-1}, pH was 7.5, and temperature was 20 °C. Biological filter in the ABTOW was fed on the modified liquid medium (g L^{-1}): $(NH_4)_2SO_4$ 0.5, KH_2PO_4 0.2, $CaCl_2$ 0.016, $MgSO_4 \cdot 7H_2O$ 0.04, $NaHCO_3$ 0.12.

2.2. Bacteria immobilization in the calcium alginate

Nitrifying bacteria were harvested by centrifugation (9000 rpm, 50 min) of 0.5 L of the bacterial culture. The pellet was mixed with 100 mL of 2% sodium alginate for bacteria dispersion. The suspension was instilled into the 4% solution of $CaCl_2$ (4 °C). In this way, bacteria were trapped in the calcium alginate spheres (±3 mm diameter). Material was stored in 4 °C, and the nitrification activity was maintained for at least 14 d.

2.3. AOB and NOB nitrification kinetics

Consortia of nitrifying bacteria immobilized in the calcium alginate were used for the determination of standard Michaelis-Menten kinetic parameters of nitrification (Nakhla et al., 2006). Oxygen consumption by bacteria was used as an estimator of the nitrification rate. The consumption was measured in 100 mL closed chamber on the magnetic stirrer and the oxygen electrode dipped in medium with immobilized biomass. Rate of nitrification was defined as first derivative (taken at 0) of a square function of time, describing the magnitude of oxygen consumption. On the basis of those data, half-saturation constants $K_{m(AOB)}$, $K_{m(NOB)}$ and nitrification rates V_{AOB}, V_{NOB} were determined using iteration method with quasi-Newton algorithm (Statistica 8.0 Statsoft, US).

2.4. Biofilm bioreactor system

Biofilms have grown in the cylindrical-shaped OCPM (length 100 mm, diameter 25 mm) in the 120 mm long polystyrene tube of 25 mm diameter. Bioreactor was placed in a horizontal position (Fig. 1a). The constant laminar flow velocity (u) equal to 0.0037 m s^{-1} (100 mL min^{-1}) was maintained with a laminar pump. Biofilm activity was monitored using two oxygen sensors on both ends of the bioreactor (as described later). The system in-

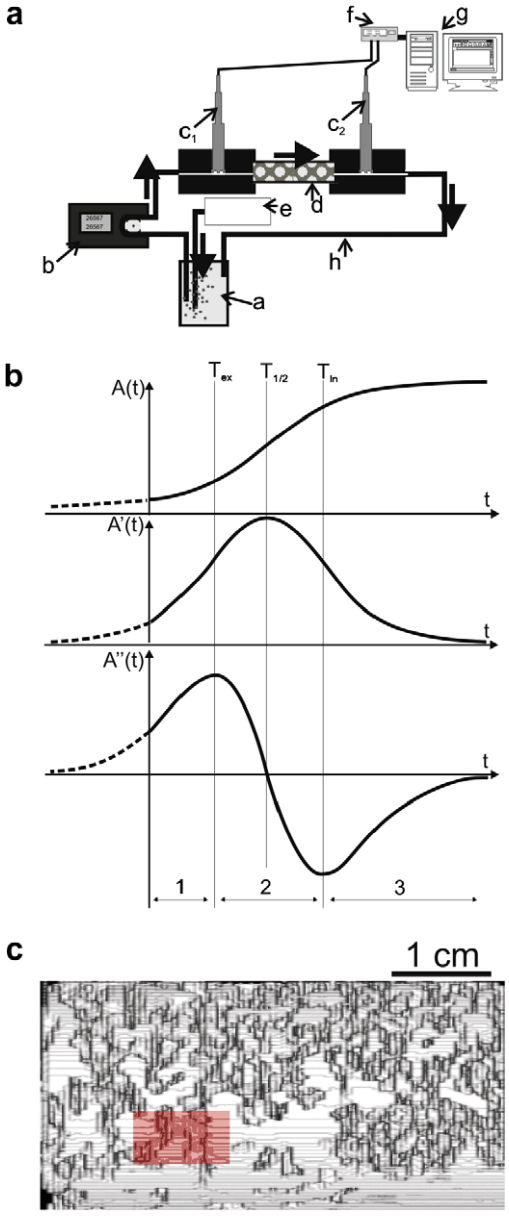

Fig. 1. (a) Scheme of ABTOW bioreactor. The main components, described with thin arrows, as following: a – nutrient and mixing chamber, b – peristaltic pump, c – oxygen electrode, d – foam reactor, e – air pump, f – transducer, g – data registrating computer, h – recirculation loop. Direction of the flow (air and water) is marked with thick arrows, (b) Verhulst model: $A(t)$ – changes in bioreactor activity, $A'(t)$ – rate of bioreactor activity changes, $A''(t)$ – acceleration of bioreactor activity changes section (1) is the exponential stage increasing an activity, section (2) is the linear stage, section (3) is the logarithmic stage. X-ray tomography image of 28 d biofilm. (c) Red box shown in the region of probe collection.

cluded a mixing chamber designed for medium aeration and nutrient addition. The water temperature in the reactor system was maintained at 22 °C.

2.5. Bacteria immobilization and growth in bioreactor

Bioreactor made by OCPM was used for bacteria immobilization in the ABTOW. Bacterial (100 mL) culture from fed-batch culture was centrifuged (RCF 15,000*g* per 50 min) with Janetzky K24 centrifuge. Harvested biomass was suspended in 100 mL of nutrient solution. Initial activity of the biomass was determined as the oxygen consumption rate during incubation in the stationary system and was equal to 1.19 ± 0.01 μmol min^{-1}. The biomass with the nutrient solution was then pumped through the reactor with the laminar flow $u = 0.0037$ m s^{-1} (100 mL min^{-1}) by 24 h in the close system. This was followed by pumping of 10 L of aerated water (4 L air min^{-1}) containing the nutrient ingredients through the system for 28 d. During experiment, level of ammonium in the medium was adjusted daily to 7.6 mM.

2.6. Chemical analysis

Nitrate was examined using brucine method (APHA, 1975). The respective millimolar absorption coefficient (410 nm) was 1.14 cm^{-1}. Nitrite was examined spectrophotometrically with α-naphthylamine and sulphanilic (APHA, 1995), and the millimolar absorptive coefficient (520 nm) was 41 cm^{-1}. Ammonium was examined using Nessler method (APHA, 1975), and the millimolar absorptive coefficient (410 nm) was 0.81 cm^{-1}. All measurements were taken using Helions ε spectrophotometer (Thermo Scientific, US).

2.7. Ion chromatography analysis

For nitrite, nitrate and phosphate anions speciation in the medium, IC 761 Compact equipped with column METROSEP A SUPP 56.1006.520 (dimension 4.0 mm × 150 mm) and conductivity detector was used. Carbonate buffer (1.0 mM $NaHCO_3$ and 3.2 mM Na_2CO_3) was used as an eluent with flow rate 0.7 mL min^{-1}, the column temperature was 20 °C, the pressure 7.7 MPa and the injection volume 20 mL.

2.8. X-ray computed tomography

Control OCPM and OCPM with biofilm were embedded in the plastic tube and were examined using X-ray tomograph (Bright Speed S BS01, GE medical system). The machine was equipped with 0.625/5.62 head and operated at 80 kV and 9 mA. A total of 89 cross sections through OCPM were computed from the X-ray data. The control OCPM and OCPM with biofilm were visualized and particle analyzed using WCIF ImageJ 1.32a.

2.9. Determination of bacteria metabolic activity in bulk

Prior to the experiments, the dependence of the rate of nitrification on the concentration of the substrates was measured. Concentration ranges of 0–8 mM of ammonia and 0–30 mM nitrite were examined (Supplementary material Fig. S1a and b). The nitrification velocity followed kinetics Michaelis-Menten kinetic (Table 1). For measuring daily maximum bacterial activity, specific substrates for AOB and NOB 7 mM ammonium or 15 mM nitrite were selected so that the respective activities were equal to V_{max} (Table 1).

The activity ($A(t)$) was measured as a difference between oxygen concentrations in the inlet and outlet of bioreactor (oxygen consumption) as a function of time. The oxygen level in the water was measured with galvanic electrodes Senco CTN-9202 S with 90% response time less than 30 s and accuracy at least 0.1 mg L^{-1}. The measurements were taken at 10 s intervals using a digital transducer (Woznica et al., 2006). Averages of 60 measurements were taken as activity estimators. The reactor was daily washed by distilled water for 20 min to wash out all nutrients. Electrode readings in distilled water were the reference points to oxygen concentration calculation during experiment. To determine daily activity, AOB and NOB were measured independently using standard medium with ammonium (AOB) or nitrite (NOB). The medium was pumped in the open cycle (the effluent medium was removed) through reactor for 15 min each for the estimation AOB/NOB oxygen consumption.

Table 1
Kinetic parameters of AOB and NOB growth for consortia of nitrifying bacteria immobilized in the calcium alginate, determined using iteration method with quasi-Newton algorithm (Statistica 8.0 Statsoft, US).

Parameter	Symbol	Unit	AOB	NOB
Half-saturation constant	K_m	mM	1.06	0.39
Oxygen uptake rate	V_{max}	μmol min^{-1}	36	15
Optimum pH	–	–	7.1–7.8	7.3–8.4
Q_{10}[a]	Q_{10}[b]	–	1.58	
Optimal temperature[a]	T_{opt}	°C	20–25	

[a] Q_{10} and optimal process temperature T_{opt} were measured for both stages of nitrification.
[b] Q_{10} were calculated for 10 and 20 °C.

One might expect (according to the data regarding the AOB activity, Table 1) that approximately 7.6 μmol of nitrite was produced during the time corresponding to the complete medium exchange in the bioreactor (approximately 30 s). That amount of substrate corresponded, in turn, to 0.14 μmol of oxygen consumption by NOB (see Table 1), which constituted less than 0.5% of total oxygen consumption in these conditions (and may be omitted).

It should be noted that the activities negligible (i.e. was within measurement error) when nitrification substrates (ammonia or nitrate) were omitted. Thus, possible presence of other than the nitrifying bacteria in the bioreactor did not contribute to the overall activity in our system.

2.10. Bacteria activity evaluation

The activities of AOB/NOB oxygen consumption (A) were described by Verhulst (logistic) model (Fig. 1b and Eqs. (1), (2))

$$\frac{dA}{dt} = \mu A\left(1 - \frac{A}{A_m}\right) \tag{1}$$

where μ is the specific rate of activity increase (d^{-1}), A_m is the maximum activity.

The solution of Eq. (1) is:

$$A(t) = \frac{A_m}{1 + d_A e^{-\mu t}} \tag{2}$$

d_A is the relative activity increase in an arbitrary constant that may be calculated from $[A_m - A_0]/A_0$, where: A_0 is initial activity at $t = 0$.

From Eq. (2), characteristic points were calculated: T_{ex} is final time of the exponential activity increasing, $T_{1/2}$ is time at which the activity is increasing at the fastest rate (when $A(t)$ is equal to one half A_m), T_{ln} is initial time of the logarithmic activity increasing (Fig. 1b). The parameters A_m, d_A, μ in the function $A(t)$ estimated numerically by fitting Eq. (2) to the empirical data with Levenberg–Marquardt algorithm implemented in Statistica 8.0 (Statsoft, US).

2.11. Quantification of AOB and NOB in the biofilm using fluorescence in situ hybridization (FISH)

Samples of the biofilm (50 μL, weakly attached to the OCPM) were collected every 2 d with the use of a pipette (end of tips wide ca 1.5 mm diameter). The biofilm was acquired at 0.5–1.0 cm from the bottom and 1.0–2.0 cm from the front of the bioreactor. The region of sampling (shown with red spot[1] in the Fig. 1c) was localized within main body of the biofilm in the bioreactor, as verified using X-ray computed tomography. Samples of biofilm were transferred to a microscopic slide, and fluorescent labelling of the nitrifying bacteria was performed. The AOB and the NOB were detected in the biofilm by fluorescence in situ hybridization using commercially available Nitri-VIT kits (vermicon AG, Germany). Nitri-VIT® contains a mixture of oligonucleotide DNA probes complementary to specific 16S rRNA regions of described AOB from environmental fresh water samples (detected genera: *Nitrosomonas, Nitrosococcus, Nitrosospira*) and NOB (detected genera: *Nitrobacter, Nitrospira*). The probe sequence specificities were validated in silico using the function "probe match" of the software package arb (Ludwig et al., 2004) and the latest arb SILVA database for rRNA sequences version 96, released 2008 (Pruesse et al., 2007). Moreover, hybridization efficiencies were validated in situ on a panel of AOB and NOB pure cultures (Supplementary material Tables S1 and S2).

These data indicate that the hybridization efficiencies of the used probes for nitrifying bacteria were close to 100%, whereas non-specific hybridization signals were not detectable with other bacteria. The labelling was executed according to manufacturer's instructions. The eubacterial (EUB) oligonucleotide probe mixture (Daims et al., 1999) complementary to a region of 16S rRNA common for all bacteria was applied as a positive control, whereas no probe was added in the negative control of the Nitri-VIT® kit. The AOB fluorescence (excitation 475–500 nm, emission 510–560 nm) and NOB fluorescence (excitation 530–550 nm, emission 570–610 nm) were registered using a SCAN^R imaging cytometer (Olympus, Poland). Distinct populations of AOB and NOB were counted after hybridization. The cytometer (build on Olympus IX inverted microscope) was equipped with stabilized 100 W Xenon burner (Olympus MT 20 illuminator), 60× PlanApo oil immersion (NA = 1.4) objective (total optical magnification of the system was equal to that of the objective), a Hamamatsu Orca AG cooled (to −30 °C) monochrome charge-coupled device camera (pixel size 6.45 μm) and a motorized stage (Marhauser, Germany). Series of 15 images corresponding to each of the two fluorescence bands were collected at different depths (−14 to 14 μm from the reference plane, 2 μm step) from each region (from 100 to 150) in a specimen (sample, positive and negative control corresponding to a given biofilm growth time). The regions (fields of view) were changed in automatic fashion using motorized stage, and the reference plane was determined using software autofocus (maximum average gradient, AOB fluorescence band). No image was registered if a field of view contained no biofilm. Fluorescence images (1364 × 1024 pixels, no binning) were collected with 200 ms (AOB) or 500 ms (NOB) acquisition time and digitized with 12 bit precision (4096 intensity levels). The image acquisition was controlled using SCAN^R acquisition software.

2.12. Image processing and analysis

Maximum depth (z) projections of the image series were generated in order to obtain sharp image of bacteria clusters positioned at different depths in biofilm. The areas occupied by biofilm (comprising bacteria and extracellular matrix, EPS) were isolated using global thresholding of images corresponding to AOB fluorescence. The threshold value was chosen to be higher than 99th percentile of fluorescence intensity in corresponding band of negative control and verified using positive control. Therefore, the isolated areas corresponded to the bacteria (stained specifically by FISH) and the EPS (exhibiting non-specific staining) but did not include regions where only instrumental background signal was present. It should be noted that the fluorescence of EPS was uniform and lower that that of the bacteria. Thus, the bacteria corresponded to bright, textured regions detectable against the dimmer EPS background. The images corresponding to AOB and NOB were subjected to rank (minimum) levelling to eliminate the EPS signal. The mask size (75 pixels) was chosen so as to preserve the signal corresponding to the largest clusters of the respective kinds of bacteria. The clusters were then segmented using global thresholding (the threshold value calculated with Otsu algorithm using all images corresponding to a specimen). The clusters were then assigned to areas occupied by the biofilm (isolated in the first step). The relative participation of the AOB and the NOB in the biofilm (area fraction) was calculated as the ratio of the areas occupied by the bacteria aggregates (estimated in the second step) to the total area of the biofilm (estimated in the first step).

3. Results

3.1. Determination of parameters of nitrification kinetics

To optimize the conditions of AOB and NOB cultures, the dynamics of oxygen consumption in the initial inoculum was determined. Kinetic data (K_m and V_{max} and optimal pH) shown in Table 1 indicated that activity of AOB in the inoculums was higher than that of NOB. Moreover, the values of maximal rates (V_{max}) indicated that in the balanced bioreactor containing both groups (AOB and NOB) of nitrifying bacteria, the AOB oxygen uptake would dominate being two times higher than that of NOB. This notion was compatible with the complete ammonium oxidation process stoichiometry.

Both groups of bacteria (AOB and NOB) preferred alkaline conditions, when pH was higher than 7.1 or 7.3, respectively. However, ammonium metabolism caused acidification of medium and subsequent decrease of the activity. When pH was 6, activity of both groups of bacteria decreased to about 15% of maximum. Increase in the optimum temperature during the ammonium nitrification indicated mesophilic character of this process (Table 1).

Changes in medium composition during the biofilm development are shown in Fig. 2. Concentrations of ammonium, nitrite and nitrate and pH of medium in bioreactor were monitored daily (Fig. 2a and c). The pH was daily corrected (as described in Section 2.). The pH was correlated with nitrification activity (the Pearson's correlation coefficient – PCC – was 0.75) and oxygen consumption (PCC was 0.94) (Fig. 2d). Changes in concentration of nitrite and nitrate in the medium indicate that both AOB and NOB were present in the biofilm (Fig. 2a). Nitrite that appeared in the medium was absorbed by NOB and oxidized to nitrate. Therefore, real production of this intermediate of nitrification process was a product of its synthesis and consumption. One may note that only low level of nitrite was observed in the medium. NOB activity in the period between 1 and 17 d of experiment was slower than nitrite production. After 17 d, steady state was reached, and all nitrite was metabolized in real time.

During experiment, decrease in phosphate concentration in the medium was observed. It correlated with nitrate production in negative manner (PCC was −0.89). Therefore, in that kind of system, one may use phosphate as the indicator of bacterial growth (Fig. 2b).

[1] For interpretation of color in Fig. 1, the reader is referred to the web version of this article.

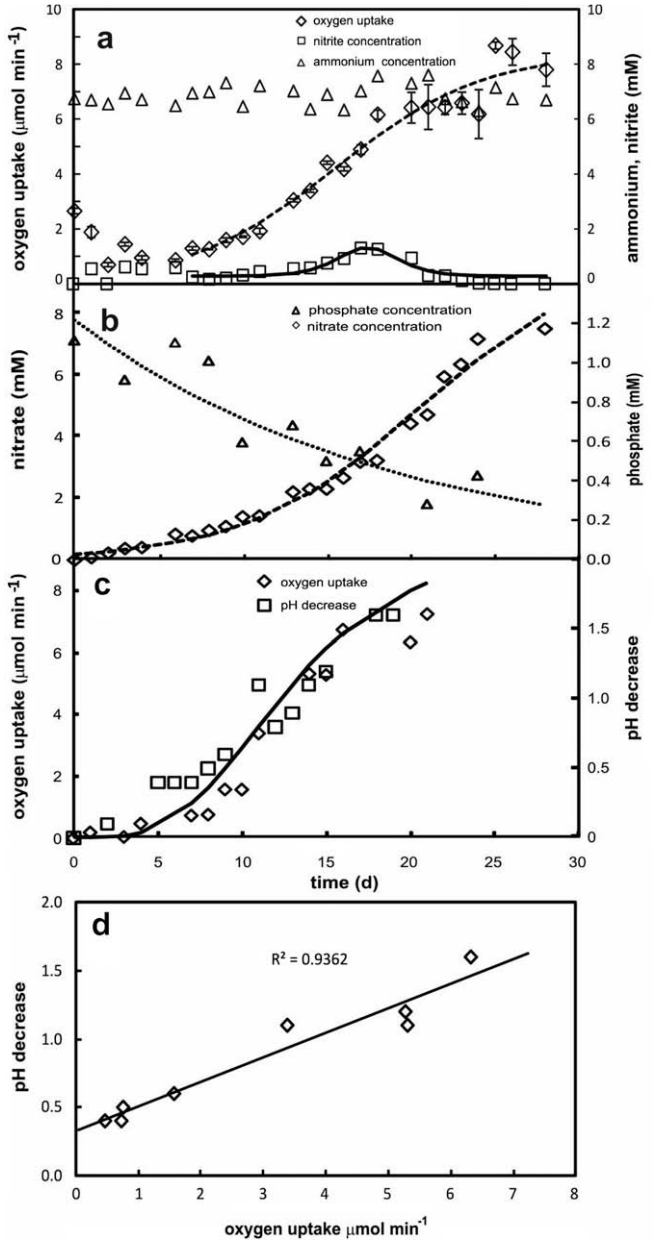

Fig. 2. Ions speciation in the medium flowing through the bioreactor a and b, oxygen uptake and daily pH decrease c, correlation between pH decrease and oxygen uptake d.

3.2. Monitoring AOB and NOB activity changes during sponge colonization

The total activity of AOB and NOB (estimated with oxygen consumption) was measured in the periodic reactor. After immobilization on the OCPM, the bacteria activity of AOB and NOB decreased (Fig. 3a). From 7th d on, an increase in the activity was observed to reach plateau on the 25 d. This process was modelled using logistic (Verhulst) equation (Fig. 3a, top), as described in Section 2.

3.3. Ammonium oxidizing evaluation

The AOB activity was measured using ammonium as electron donor. It should be noted that nitrite concentration in the medium during the measurement was very low and therefore possible NOB activity did not contribute to the oxygen consumption in these

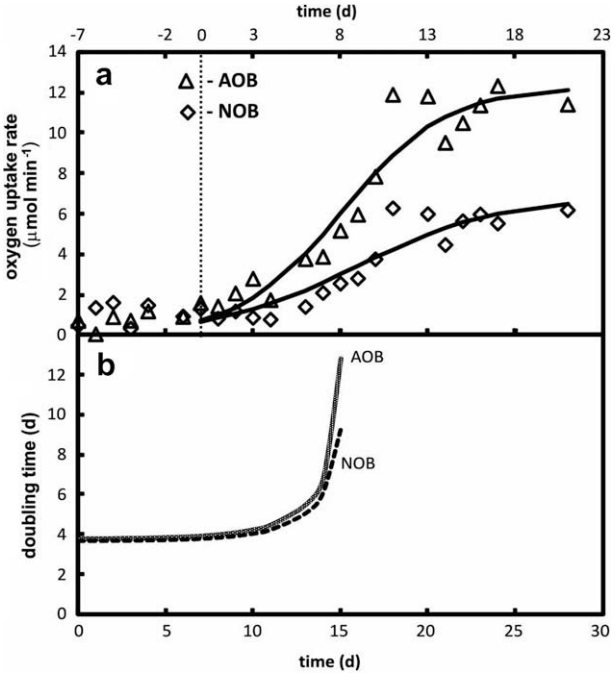

Fig. 3. Change of AOB and NOB activity measured as a rate of oxygen uptake in the bioreactor ABTOW during bacteria growth (a), calculated doubling activity time (DT) of biofilm activity for AOB and NOB in the bioreactor (b).

conditions. Changes in the AOB activity during biofilm development were modelled using logistic function (see Section 2). The relevant parameters are shown in Table 2. Three critical points were observed in the growth of AOB activity. The first was in the 11th d of experiment (maximum of second derivative function) when activity started to increase rapidly (Fig. 3a). The second was in the 15th d of experiment – when growth rate started to decrease (maximum point of first derivative function) – and the third was in the 21st d of experiment when the activity began to stabilize (minimum of second derivative function). During first 9 d, average doubling time of bacterial activity (DT) was about 4.3 ± 0.02 d. In the 10th d of experiment, DT started to increase and in the 15th d reached 13 d (see Fig. 3b).

3.4. Nitrite oxidizing evaluation

The NOB activity (with nitrite as electron donor) was measured in a similar fashion to the AOB activity. We observed increase in the NOB activity during biofilm development, but its maximum (6.84 μmol min^{-1}) was lower than the corresponding value for AOB. However, similar to AOB, the increase could be modelled using logistic function (Table 2 and Fig. 3a). One may note that the DT (in the first 9 d of experiment) of NOB (DT_{NOB}) was similar

Table 2
Parameter of Verhulst function. The parameters A_m, d_A, μ were estimated numerically by fitting Eq. (2) to the empirical data with Levenberg–Marquardt algorithm implemented in Statistica 8.0 (Statsoft, US).

Parameter	Unit	AOB	NOB
A_{max} (from fitting)	μmol min^{-1}	12.3	6.2
A_0 (from measurements)	μmol min^{-1}	1.30	1.57
μ (from fitting)	d^{-1}	0.41	0.43
d_A (from fitting)	-	19.4	25.1
$T_{1/2}$ (from calculations)	d	7.3	7.4
T_{ex} (from calculations)	d	4.0	4.4
T_{ln} (from calculations)	d	10.5	10.5

to the respective value for AOB (DT_{AOB}) and corresponded, on average, to 3.9 ± 0.1 d. Similarly, DT_{NOB} increased from 10 d reaching 9.2 d in the 15 d of the experiment (Fig. 3b).

3.5. Participation of AOB and NOB in the biofilm

The relative participation of the two groups of nitrifying bacteria in the biofilm was estimated using FISH and image cytometry (see Section 2). Change in AOB area fraction was correlated with NOB area fraction (correlation quotient 0.99, Figs. 4a–c and 5). However, AOB dominated in the biofilm during the experiment. With the exception of the first part of experiment (when total activity was low), the ratio of the values of AOB/NOB area fractions was approximately 1.85 ± 0.2 (Fig. 4b and e). One should note that similarly high correlation was observed between activities of AOB and NOB (Fig. 4f). Likewise, the ratio of activities of AOB and NOB was 2.1 ± 0.38.

During 28 d of experiment, we observed changes in the biofilm structure. Our data showed that biofilm during this time was reconstructed. In the initial phase when mature flocks from fed-batch culture were immobilized in ABTOW small size (5 μm), AOB and NOB colonies appeared together (Fig. 5a and b) in a tightly packed biofilm structure. In the 7th d, the biofilm was sparsely populated with colonies of intermediate size (8 μm) scattered in the EPS (visible as diffuse fluorescent background, Fig. 5c and d). One should note that AOB predominated whereas NOB were scarce at this stage. In the 11th d of experiment, biofilm started to mature. The diameter of colonies increased; in the 14th d of experiment the average was 25 μm (Fig. 5e–h). Moreover, on the surface of AOB colonies, groups of NOB cells appeared (Fig. 5i and j).

One should note that mature biofilm (28th d of experiment) that occupied approximately 40% of total OCPM volume (Fig. 2c) was estimated using X-ray tomography. Hence, the total biofilm volume in the bioreactor was approximately 22.7 cm^3. Taking into account proportion of biofilm volume occupied by the bacteria (determined with image cytometry), one may estimate that this volume corresponded to approximately 1.6×10^{13} AOB cells and 1.2×10^{13} NOB cells, respectively. This estimation was carried out under assumption that all the nitrifying bacteria were detected. Hence, it corresponds to the lower limit of the numbers of the AOB and NOB in the bioreactor.

4. Discussion

Application of the biofilter (bacterial biofilm immobilized on the OCPM) for biosensing requires that stability of the biofilm structure and its biocatalytic activity (maintained by homeostasis) are ascertained. Using imaging techniques combined with bulk activity measurements, one may conclude that in the presented ABTOW such stability is reached 21 d after inoculation. This point

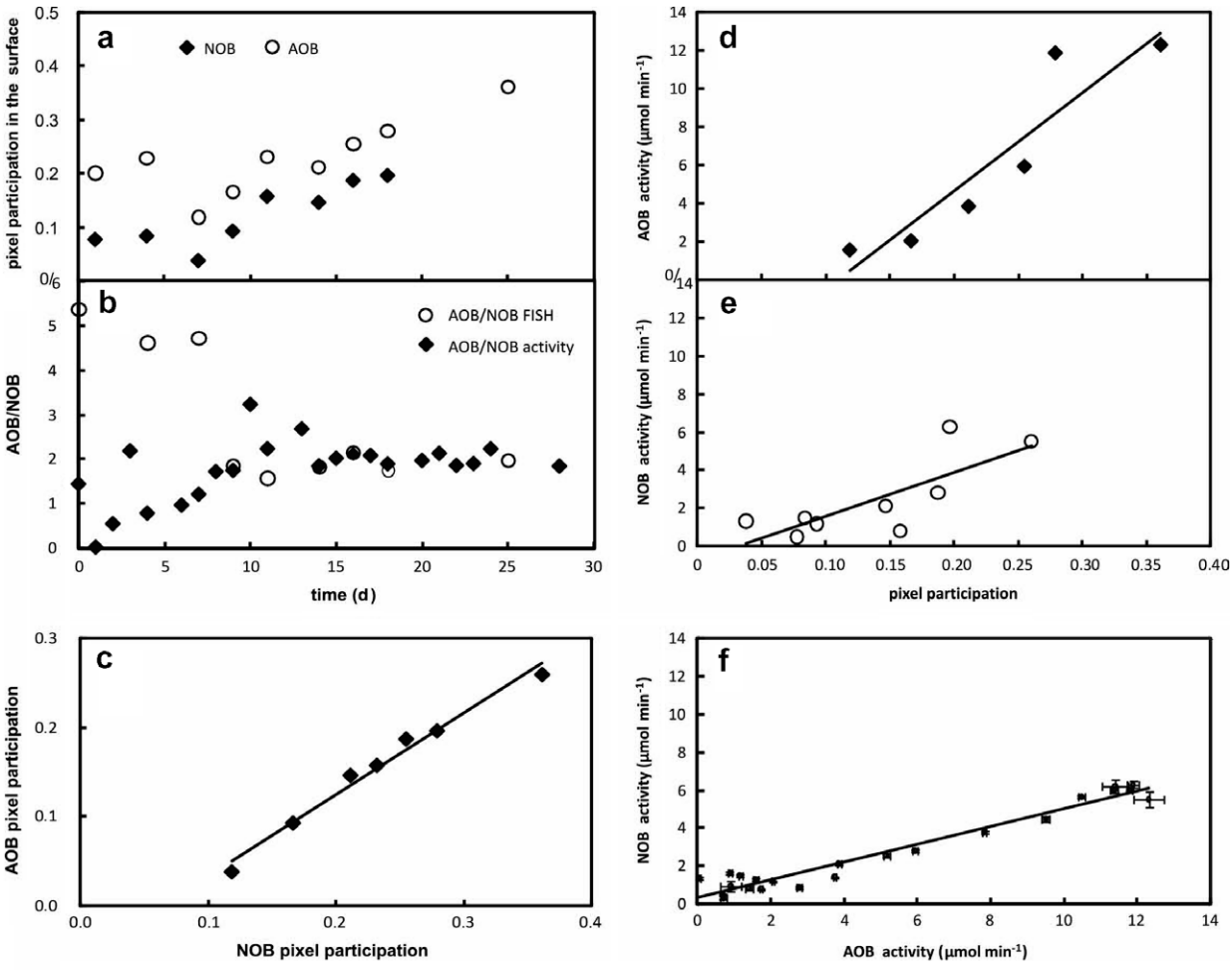

Fig. 4. Bioreactor activity and AOB & NOB pixel participation in the OCPM during biofilm maturation. a – AOB and NOB pixel participation on the analyzed surface; b – proportion between AOB/NOB pixel participation and AOB/NOB activity in the time; c – correlation between AOB and NOB pixel participation; d – correlation between AOB activity and AOB pixel participation; e - correlation between NOB activity and NOB pixel participation; f – correlation between AOB and NOB activity.

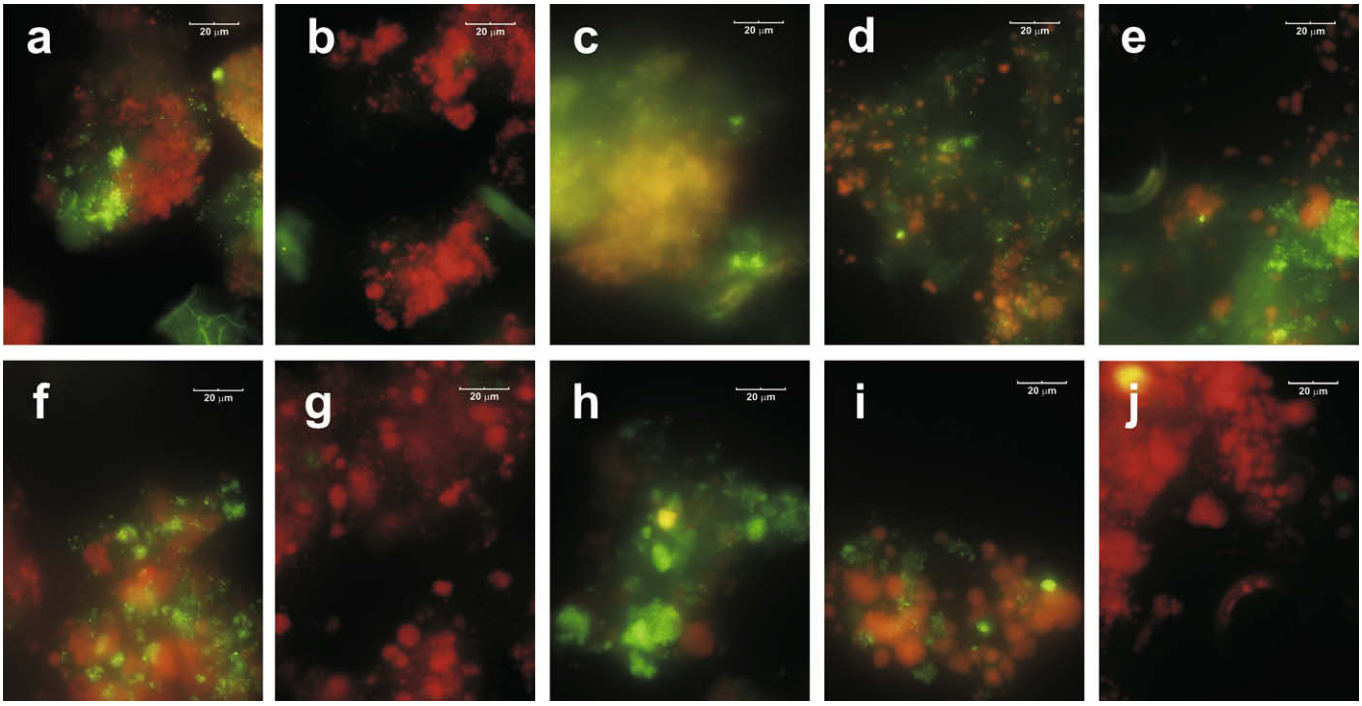

Fig. 5. Microscope image of FISH labelling nitrifying bacteria biofilm: AOB (red) and NOB (green) in the OCPM in the 1 (a), 4 (b), 7 (c), 9 (d), 11 (e), 14 (f), 16 (g), 18 (h), 22 (i), 25 (j) day of experiment.

corresponds to biofilm containing large microbial flocks containing both AOB and NOB colonies. Interestingly, no nitrite in the medium was observed at this stage. One may hypothesize that in matured floccules the nitrite produced by confluent AOB was cumulated in the flocks. Increase in the nitrite level stimulated the activity of NOB (localized on the external surface of AOB microcolonies) that consumed this compound in full. Therefore, nitrite appeared in the medium only when AOB/NOB proportion was not balanced (i.e. in immature biofilm).

One might imagine that the procedure of estimation of average density of packing of bacteria within the biofilm with an imaging technique could be affected by the penetration of the FISH probes into the biofilm and possible low affinity of the probe to the bacterial rRNA. We did not detect any non-uniformity of the non-specific matrix staining with the depth in the biofilm (the samples were at most 20 μm thick in our system). Moreover, we were able to detect FISH signals from 75 μm depth into the biofilm with confocal microscopy. Therefore, the first problem is unlikely to affect the results in our system. Nonetheless, some bacteria might escape detection if their specific fluorescence (following FISH) was too weak. It should be noted, however, that our system was sensitive enough to detect bacterial autofluorescence. Moreover, according to the manufacturer, significantly higher FISH signals were detectable in all tested target species of nitrifying bacteria. However, it seems unlikely that a putative species (characterized by low efficiency of FISH reaction) constituted a significant part of nitrification population in our system and markedly affected the presented results owing to the in silico and in situ tested specificity of probes.

The stabilization of biofilm structure and activity implies the existence of a limiting factor of bacterial growth. It may be postulated that oxygen played that role. The oxygen concentration in the water flowing through the bioreactor decreased owing to bacterial activity. The decrease corresponded to 5% of oxygen content (in equilibrium with atmospheric air) at the onset of incubation and 50% in the 20 d of the experiment, respectively. This notion is in agreement with the fact that the volume of sponge occupied by biofilm decreases with the distance from bioreactor inlet, as established using X-ray tomography. One should note that availability of oxygen in the interiors of large flocks (Fig. 5h–j) could be decreased (owing to limited its diffusion) thereby constituting constraint of bacterial growth.

The biofilm growth and stabilization of its activity were modelled using Verhulst (logistic) equation. This model was chosen because it provided a good fit to the experimental data while maintaining low numerical complexity. The three parameters of the model – A_{max}, μ and $T_{1/2}$ – could be easily interpreted biologically. Moreover, bacterial growth rate could be estimated with DT calculation. The Verhulst model also permitted analytical calculation of the first and the second derivatives that offered additional insight into the biofilm growth (Table 2).

The biofilm activity was monitored using ammonia or nitrite concentrations that corresponded to maximum rate of the nitrification (see Section 2). The results presented in (Anthonisen et al., 1976) indicate that (in the continuous flow conditions) the concentration of free ammonia corresponding to our experimental conditions (0.748 mg L^{-1} FA) was sufficient to cause some inhibition of nitrification (in majority of experiments). One may note that the respective half-saturation constants K_m (Table 1) were significantly smaller than inhibition thresholds reported by (Anthonisen et al., 1976). Furthermore, no changes in activity were observed when V_{max} (and potential inhibition threshold) was reached. Thus, one may postulate that the change of nitrification rate with substrate concentration reflected saturation of respective enzymes and not their inhibition by free ammonia or free nitrous acid.

It may be noted that the kinetic parameters (Table 1) correspond to the total volume of the biofilm in the proposed ABTOW. Direct estimation of the biomass of a delicate biofilm in 3D system is difficult owing to possible losses in extraction of the biomaterial, irregular distribution of biofilm in the OCPM and the presence of several different forms of immobilization. Therefore, the total volume of the biofilm could be determined only indirectly using X-ray tomography.

One should note that such system used as a biodetector high sensitivity of toxin detection in water environment. For example,

the lowest observed effect levels were 10 μM for phenol and 0.1 μM for cyanide (in water) when the ABTOW described in this work was used (data not shown). This high sensitivity is stably maintained during 4–6 weeks of operation of the ABTOW. Moreover, this biodetector exhibits short response lag (approximately 1.5 min) while measurements may be taken in real time and on continuous basis. Up to 100 mL min^{-1} of water sample may be measured in this manner in situ owing to the fact that OCPM provided low resistance to flowing water. Therefore, it may be concluded that OCPM provided good basis for immobilization of nitrifying bacteria as biosensing element.

Nonetheless, long generation time (due to slow growth rates of nitrifying bacteria in this system) may be regarded as disadvantage to industrial-scale production of such sensors. On the other hand, slow change of the number of bacteria in the biofilm and consequently its biological activity provide good stability of the biodetector. Moreover, once biofilm is matured, these characteristics will prevent overgrowing of the biofilters, thereby extending life span of such biosensor.

Acknowledgments

Special thanks are due to Aleksander Gmur from District Hospital, Pszczyna, to Jagna Karcz from Laboratory of Scanning Electron Microscopy, Faculty of Biology and Environmental Protection. This work was supported by the Polish Ministry for Science and Higher Education (MNiSW) Grant No. N N301 463834.

Appendix A. Supplementary material

Supplementary data associated with this article can be found, in the online version, at doi:10.1016/j.chemosphere.2009.12.035.

References

Al-Raoush, R.I., Willson, C.S., 2005. Extraction of physically realistic pore network properties from three-dimensional synchrotron X-ray microtomography images of unconsolidated porous media systems. J. Hydrol. 300, 44–64.

Anthonisen, A.C., Loehr, R.C., Pracasam, T.B.S., Srinath, E.G., 1976. Inhibition of nitrification by ammonia and nitrous acid. J. Water Pollut. Control Fed. 48, 835–852.

APHA, 1975. Standard Methods for the Examination of Water and Wastewater, 14th ed. American Public Health Association, Washington, DC.

APHA, 1995. Standard Methods for the Examination of Water and Wastewater, 19th ed. American Public Health Association, Washington, DC.

Bang, S.S., Galinat, J.K., Ramakrishnan, V., 2001. Calcite precipitation induced by polyurethane-immobilized *Bacillus pasteurii*. Enzyme Microb. Technol. 28, 404–409.

Bettaieb, F., Ponsonnet, L., Lejeune, P., Ouada, H.B., Martelet, C., Bakhrouf, A., Jaffrézic-Renault, N., Othmane, A., 2007. Immobilization of *E. Coli* bacteria in three-dimensional matrices for ISFET biosensor design. Bioelectrochemistry 71, 118–125.

Blum, L.J., 1997. Bio- and Chemi-Luminescent Sensors. World Scientific, Singapore.

Bothe, H., Jost, G., Schloter, M., Ward, B.B., Witzel, K.P., 2000. Molecular analysis of ammonia oxidation and denitrification in natural environments. FEMS Microbiol. Rev. 24, 673–690.

Chandran, K., Love, N.G., 2008. Physiological state, growth mode, and oxidative stress play a role in Cd(II)-mediated inhibition of *Nitrosomonas europaea* 19718. Appl. Environ. Microbiol. 74, 2447–2453.

Christensen, T.H., Cossu, R., Stegmann, R., 1992. Landfilling of Waste: Leachate. Taylor & Francis, London.

Cui, R., Chung, W.J., Jang, D., 2005. A rapid and simple respirometric biosensor with immobilized cells of *Nitrosomonas europaea* for detecting inhibitors of ammonia oxidation. Biosens. Bioelectron. 20, 1788–1795.

de Ory, I., Romero, L.E., Cantero, D., 2004. Optimization of immobilization conditions for vinegar production. Siran, wood chips and polyurethane foam as carriers for *Acetobacter aceti*. Process Biochem. 39, 547–555.

Daims, H., Brühl, A., Amann, R., Schleifer, K.-H., Wagner, M., 1999. The Domain-specific probe EUB338 is insufficient for the detection of all bacteria: development and evaluation of a more comprehensive probe set. Syst. Appl. Microbiol. 22, 434–444.

Diaz, C., Lelong, P., Dieu, P., Feuillerat, C., Salome, M., 1999. On-line analysis and modeling of microbial growth using a hybrid system approach. Process Biochem. 34, 39–47.

Fujikawa, H., Kai, A., Morozami, S., 2004. A new logistic model for *Escherichia coli* growth at constant and dynamic temperatures. Food Microbiol. 21, 501–509.

Gieseke, A., Purkhold, U., Wagner, M., Amann, R., Schramm, A., 2001. Community Structure and activity dynamics of nitrifying bacteria in a phosphate-removing biofilm. Appl. Environ. Microbiol. 67, 1351–1362.

Hovanec, T.A., Taylor, L.T., Blakis, A., Delong, E.F., 1998. Nitrospira-like bacteria associated with nitrite oxidation in freshwater aquaria. Appl. Environ. Microbiol. 64, 258–264.

Ilzumi, T., Mizumoto, M., Nakamura, K., 1998. A bioluminescence assay using *Nitrosomonas europaea* for rapid and sensitive detection of nitrification inhibitors. Appl. Environ. Microbiol. 64, 3656–3662.

Kahru, A., Dubourguier, H.C., Blinova, I., Ivask, A., Kasemets, K., 2008. Biotests and biosensors for ecotoxicology of metal oxide nanoparticles: a minireview. Sensors 8, 5153–5170.

Kim, Y.M., Park, D., Lee, D.S., Park, J.M., 2008. Inhibitory effects of toxic compounds on nitrification process for cokes wastewater treatment. J. Hazard. Mater. 152, 915–921.

König, A., Riedel, K., Metzger, J.W., 1998. A microbial sensor for detecting inhibitors of nitrification in wastewater. Biosens. Bioelectron. 13, 869–874.

Koops, H.P., Pommerening-Röser, A., 2001. Distribution and ecophysiology of the nitrifying bacteria emphasizing cultured species. FEMS Microbiol. Ecol. 37, 1–9.

Kowalchuk, G.A., Stephen, J.R., 2001. Ammonia-oxidizing bacteria: a model for molecular microbial ecology. Annu. Rev. Microbiol. 55, 485–529.

Liu, Y., 2006. A simple thermodynamic approach for derivation of a general Monod equation for microbial growth. Biochem. Eng. J. 31, 102–105.

Liu, Y., Tay, J.H., 2001. Factors affecting nitrite build-up in nitrifying biofilm reactor. J. Environ. Sci. Health A 36, 1027–1040.

Lokshina, L.Y.A., Vavilin, V.A., Kettunen, R.H., Rintala, J.A., Holliger, C.H., Nozhevnikova, A.N., 2001. Evaluation of kinetic coefficients using integrated Monod and Haldane models for low-temperature acetoclastic methanogenesis. Water Res. 35, 2913–2922.

Ludwig, W., Strunk, O., Westram, R., Richter, L., Meier, H., Yadhumakar, Buchner.A., Lai, T., Steppi, S., Jobb, G., Förster, W., Brettske, I., Gerber, S., Ginhart, A., Gross, O., Grumann, S., Hermann, S., Jost, R., König, A., Liss, T., Lümann, R., May, M., Nonhoff, B., Reichel, B., Strehlow, R., Stamatakis, A., Stuckmann, N., Vilbig, A., Lenke, M., Ludwig, T., Bode, A., Schleifer, K.-H., 2004. ARB: a software environment for sequence data. Nucl. Acids Res. 32, 1363–1371.

MacDonald, R.M., Spokes, J.R., 1980. A selective and diagnostic medium for ammonia oxidizing bacteria. FEMS Microbiol. Lett. 8, 143–145.

Mota, C., Head, M.A., Ridenoure, J.A., Cheng, J.J., de los Reyes, I.I.I.F.L., 2005. Effects of aeration cycles on nitrifying bacterial populations and nitrogen removal in intermittently aerated reactors. Appl. Environ. Microbiol. 71, 8565–8572.

Nakhla, G., Liu, V., Bassi, A., 2006. Kinetic modeling of aerobic biodegradation of high oil and grease rendering wastewater. Bioresour. Technol. 97, 131–139.

Park, S., Ely, R.L., 2008. Candidate stress genes of *Nitrosomonas europaea* for monitoring inhibition of nitrification by heavy metals. Appl. Environ. Microbiol. 74, 5475–5482.

Peleg, M., Corradini, M.G., Normand, M.D., 2007. The logistic (Verhulst) model for sigmoid microbial growth curves revisited. Food Res. Int. 40, 808–818.

Pessala, P., Schultz, E., Nakari, T., Joutti, A., Herve, S., 2004. Evaluation of wastewater effluents by small-scale biotests and a fractionation procedure. Ecotoxicol. Environ. Safe. 59, 263–272.

Pruesse, E., Quast, C., Knittel, K., Fuchs, B., Ludwig, W., Peplies, J., Glöckner, F.O., 2007. SILVA: a comprehensive online resource for quality checked and aligned ribosomal RNA sequence data compatible with ARB. Nucl. Acids Res. 35 (21), 7188–7196.

Tsoularis, A., Wallace, J., 2002. Analysis of logistic growth models. Math. Biosci. 179, 21–55.

van Impe, J.F., Poschet, F., Geeraerd, A.H., Vereecken, K.M., 2005. Towards a novel class of predictive microbial growth models Int. J. Food Microbiol. 100, 97–105.

Wimpenny, J., Manz, W., Szewczyk, U., 2000. Heterogeneity in biofilms. FEMS Microbiol. Rev. 24, 661–671.

Woznica, A., Latusek, E., Płonka, A., Łabuzek, S., Duda, H., Górny, M., Klis, Cz., Kosz, K., Siudy, A., 2006. Automatic detection of water toxicity based on nitrifying bacteria biosensor. In: Proceedings of ECOpole International Conference. Society of Ecological Chemistry and Engineering, Opole.

Xi, C., Marks, D., Schlachter, S., Luo, W., Boppart, S.A., 2006. High-resolution three-dimensional imaging of biofilm development using optical coherence tomography. J. Biomed. Opt. 11 (034001), 1–6.